The shear adhesion strength between the FRC substructure and denture base resin: Effects of FRC architecture, adhesive composition and hydrolytic degradation

Petr Polacek [a,*], Michaela Salajkova [c], Josef Jancar [a,b]

[a] Central European Institute of Technology (CEITEC), Brno University of Technology, 612 00 Brno, Czech Republic
[b] Institute of Materials Chemistry, Brno University of Technology, 612 00 Brno, Czech Republic
[c] Department of Fibre and Polymer Technology, KTH Royal Institute of Technology, 100 44 Stockholm, Sweden

ARTICLE INFO

ABSTRACT

The adhesion strength between fiber reinforced composite (FRC) members and denture-base resin is pivotal for enhancing removable denture long lasting performance and patient comfort. FRC reinforcing rods based on glass fibers impregnated with light curing resin were used to model the FRC substructure. The influence of fiber architecture and adhesive layer composition on the shear adhesion strength, τ_a, between the FRC and denture-base resin was investigated both dry and in moist environment to assess the stability of the adhesive bond in the oral cavity. The obtained results suggest that for a given fiber architecture, adhesive composition and test conditions, the wetting of the FRC surface was the primary variable affecting the τ_a. In the case of good wetting and formation of adhesive bond between the substrates, interlaminar shear strength of the unidirectional FRC substrate was the limiting factor. In multi-directional FRC substrate, the shear strength of the outer resin rich layer was limiting factor for the maximum adhesion strength.

© 2013 Elsevier Ltd. All rights reserved.

1. Introduction

There is an increasing number of applications in modern dentistry using fiber reinforced composites (FRCs) in reinforcing crowns, constructing frameworks for fixed partial dentures, periodontal splints, post-orthodontic retainers, and manufacturing and repairing removable dentures as well as various acrylic orthodontic devices. Desired biomechanical performance, esthetics and patient comfort are achieved by combining easily formable load bearing FRC substructures with composite veneers, denture-base resins, flowable composites and resin based adhesives. For achieving long lasting dental device, a good adhesion between all the components is a very important prerequisite.

In addition to economical constraints, there are many clinical indications requiring replacement of missing teeth or restoring of normal function and appearance of the patient's oral cavity using removable denture. Acrylic denture base resins based on lightly cross-linked poly-methylmethacrylate (PMMA) are routinely used to manufacture removable dentures employing the "dough" technique. Easy handling, low cost, stability in the oral environment and the aesthetics are the main reasons why they became widely used. However, their limitations include low fracture toughness, poor fatigue behavior and low stiffness. Metal wires embedded in the acrylic resins are commonly used to partly obviate these deficiencies as well as to reinforce fractured dentures and other devices during their repair. Poor adhesion to the acrylic resins and poor esthetics of metal wires result in rigid, low comfort dentures prone to brittle failure. In order to address these shortcomings, FRCs have been introduced to dentistry more than a two decades ago [1]. In dentistry, various preformed FRC components replacing metal load bearing substructures or reinforcing elements are gaining popularity in a growing number of prosthetic and orthodontic applications [2–12]. Rigidity and strength of FRC are influenced by fiber type and volume fraction, fiber orientation and adhesion to the polymer matrix as well as by the quality of impregnation with the resin matrix [13].

Upon curing to the final shape, the FRC components are either covered with esthetic particulate filled composites (crowns, bridges, splints, retainers, posts) to improve patient's comfort and maintain good oral hygiene or embedded in the acrylic resin when used as reinforcing elements (removable dentures, repaired dentures, orthodontic devices) [14–17]. The quality of adhesion between the FRC substructure and the resin based esthetic materials is one of the main concerns in improving the service life of current removable prostheses and other acrylic dental devices. Since the chemistry of resins used to manufacture both dental FRCs and denture base resins is substantially similar, desired formation of

* Corresponding author. Address: Central European Institute of Technology, Brno University of Technology, Purkynova 118, 612 00 Brno, Czech Republic. Tel.: +420 541 149 495; fax: +420 541 149 361.

E-mail address: petr.polacek@ceitec.vutbr.cz (P. Polacek).

a chemical adhesive bond can be achieved [18]. However, as shown previously [19], the factors affecting the adhesion strength of a given joint also include substrate and adhesive toughness, substrate geometry, adhesive layer thickness and mode of loading the adhesive joint. Most of the published data were obtained using components cured the same way (light, heat, dual). Even though the mechanism of cure remains the same, the cure kinetics and degree of cure differ significantly for light and heat cured dental resins [20,21]. At the same time, despite its importance, little is known about the adhesion between light curing FRC and heat curing acrylic resins processed using the dough technology [22].

The addition of nanoparticles with large specific surface area (200–1000 m^2/g) compared to micrometer size fillers (0.2–5 m^2/g) into a polymer network modifies both cure kinetics and mechanical behavior below and above its glass transition temperature, T_g. It was shown that below T_g, chain packing, density fluctuations, and segmental relaxations vary proportionally to the chain–particle interface area and interfacial interaction strength similar to that observed in polymers with antiplasticizers. Nanoparticles dispersed in monomer mixtures can also self-assemble during cure into extended structures similar to colloids. Due to their extremely large specific surface area providing large interface area between the solid surface and reacting monomer mixture even at low nanoparticle content, presence of nanoparticles can affect the partitioning of reactive species in the mixture resulting in modified network structure and cure kinetics [23].

The aim of this paper was to investigate the shear adhesion strength, τ_a, between the light cured FRC substrate and lightly cross-linked, heat cured acrylic denture base resin. Nanocomposite adhesive layer with varying composition was used and the adhesion strength was investigated using modified pull-out test with varying joint geometry. To assess the longevity of the bond in the moist environment of oral cavity, joints were exposed to water for the period of up to 4 months. In addition, investigation of the loci of failure and the crack path was attempted using scanning electron microscopy (SEM) of the failed test specimens. Fracture mechanics protocol was used to analyze the experimental data.

2. Materials and methods

Commercial Bis-GMA/TEGMA monomer mixture *Evicrol* (*Kerr-Dental*, Czech Republic) was used as the resin matrix to prepare FRC rods, particulate filled composite (PFC) rings and adhesive interlayer. The photoinitiation complex consisted of 0.2 wt.% camphoroquinone (*Sigma–Aldrich*, USA) and 0.2 wt.% N,N-dimethylaminoethylmethacrylate (*Sigma–Aldrich*, USA).

FRC cylindrical rods were prepared using either continuous S2-glass roving (*AGY*, Belgium) or E-glass fiber braids (*ADM, a.s.*, Czech Republic). Fiber volume fraction, v_f, in all the FRCs investigated was kept constant at $v_f = (0.38 \pm 0.02)$. Glass fiber bundles of approximately 100 mm in length were introduced into a round clear glass tube (length approx. 40 mm, inner diameter approx. 1.5 mm). Fiber bundles protruding from the glass tube were impregnated with the monomer mixture. Then, the impregnated portion of the fiber bundle was pulled into the tube to resume its symmetrical round cross-section rod shape. The pre-impregnated fiber bundle was light cured through the glass tube using the *Targis Power* (*Ivoclar Vivadent AG*, Liechtenstein) light cure chamber for 10 min at room temperature. The sample was then removed from the tube and its surface was cleaned with acetone [24]. Round cross section braids were impregnated using the same procedure as described above.

Nanocomposite adhesive was prepared by adding desired amount of fumed silica with average particle size of 5 nm and specific surface area of 200 m^2/g (*Cab-O-Sil M-5, Cabot*, USA) into resin and mixture was vigorously stirred for 10 min at room

temperature. Three adhesive compositions with silica content of 0, 1.7 and 7.9 vol.% were prepared and stored in a dark container to prevent their premature cure.

Heat curing denture-base acrylic resin *Superacryl Plus* (*Kerr-Dental*, Czech Republic) was processed according to manufacturer's instructions. Two weight parts of the powder containing PMMA, dibutylphtalate, zinc oxide and pigments were mixed with one weight part of the liquid containing methylmethacrylate and glycoldimethacrylate to form plastic dough. The dough was processed according to manufacturer's direction and desired amount was placed into the silicon rubber mold to form the cylindrical test specimen (Fig. 1).

Reference test specimens (Fig. 1a) were prepared by placing the cured FRC rod into a rubber mold (Lukopren 1522, Lucebni zavody Kolin, Czech Republic) with a symmetrical cylindrical cavity. Rod was aligned with the axis of symmetry of the cylindrical cavity. Then, the cavity was filled with either the denture-base dough (sample group I) or adhesive (sample group II) to form a coaxial
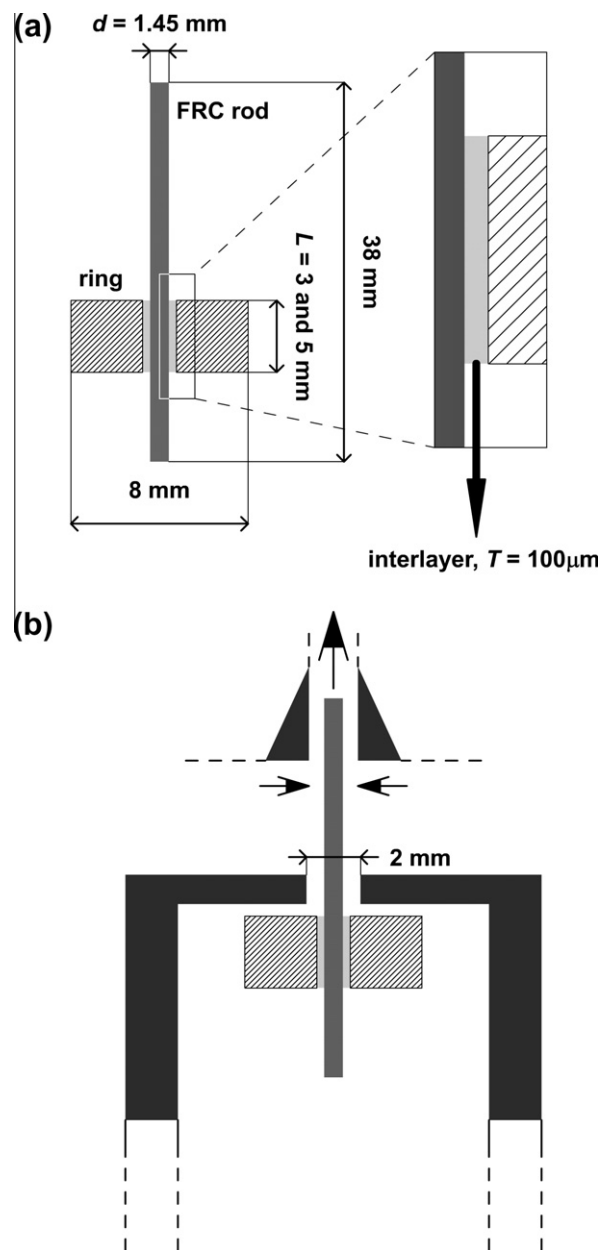
Fig. 1. (a) Dimensions of test specimen, and (b) diagram showing test geometry.

Table 1
Test specimen materials composition.

Group	Subgroup	Ring		Interlayer	
		Material	Filler content (vol.%)	Material	Filler content (vol.%)
I	SA	*Superacryl Plus*	n/a	n/a	n/a
II	E-0	*Evicrol*	0	n/a	n/a
	E-1		1.7		
	E-2		7.9		
III	SAE-0	*Superacryl Plus*	n/a	*Evicrol*	0
	SAE-1				1.7
	SAE-2				7.9
M[a]	E-0 FRC-M	*Evicrol*	0	n/a	n/a
HS[b]	SAE-0 HS RT 4 W	*Superacryl Plus*	n/a	*Evicrol*	0
	SAE-0 HS RT 4 M				
	SAE-0 HS 100 4D				

[a] FRC rod contained multidirectionally oriented fibers.
[b] HS RT 4 W, HS RT 4 M – hydrolytic stability tests at room temperature for 4 weeks and 4 months respectively, HS 100 4D – hydrolytic stability tests at 100 °C for 4 days.

Table 2
Values of adhesion strength for two joint lengths.

Group	Subgroup	Joint length, L (mm)	
		3	5
		Shear adhesion strength, τ_a (MPa)	
I	SA	3 ± 1	4 ± 1
II	E-0	28 ± 2	22.4 ± 0.8
	E-1	28.3 ± 0.7	21.6 ± 0.4
	E-2	28 ± 2	20.0 ± 1.6
III	SAE-0	12.1 ± 0.9	13.8 ± 0.5
	SAE-1	9 ± 1	9 ± 1
	SAE-2	3.8 ± 0.5	4.8 ± 0.6
M	E-0 FRC-M	21 ± 1	n/a

cylindrical ring with the FRC rod in the center. Transparent cover from transparent rubber mold was placed over the upper portion of the ring to avoid formation of a meniscus at the rod/ring interface. Test specimens made out of the adhesive were polymerized in the light curing chamber for 10 min. Specimens made of denture-base dough were polymerized in the curing oven (30 min at 70 °C and then 30 min at 110 °C under 0.6 MPa).

Test specimens with adhesive interlayer between the rod and the acrylic ring (sample group III) were prepared by placing the acrylic dough into the rubber mold with metal rod of diameter approx. 1.7 mm in the center. Metal rod was aligned with the axis of symmetry of the cylindrical cavity. The cavity was filled with dough and transparent cover was placed over the ring. Material was polymerized as described above and then, the ring was removed from the rubber mold. A Teflon tape was used to demarcate the required length of the joint on the FRC rod. Then, the cured FRC rod and the cured ring were placed into the rubber mold, aligned coaxially and the space between them was filled with the adhesive. Thickness of adhesive interlayer, *T*, was approximately *T* = 100 μm.

In total, 90 specimens were prepared. Specimens were divided into five main groups and eleven subgroups (Table 1) Four subgroups contained specimens without adhesive interlayer (sample groups I and II) and three groups contained specimens with adhesive interlayer (sample group III). In the next group, FRC rod contained multidirectional (braided) fibers instead of unidirectional fibers. (sample group M). One subgroup of test specimens was kept in distilled water at room temperature for 4 weeks, the other subgroup of specimens was kept in distilled water at room temperature for 4 months and the next subgroup of test specimens was kept in distilled water for 4 days at 100 °C to investigate hydrolytic stability of the adhesive joint (sample group HS). The influence of

the area of adhesive joint on adhesion strength was investigated using two lengths of adhesive joint (*L* = 3 and 5 mm).

Universal tensile testing machine *Zwick Z010* (*Zwick Roell*, Germany) was used to perform the pull-out tests at room temperature according to the procedure described previously [24]. Special steel clamp was used to mount the specimens (Fig. 1b). Cross head speed of 1 mm/min at room temperature was used in all measurements and the test was stopped when the rod was pulled out of the ring. Maximum stress, stress at failure and deformation at failure were recorded using the data processing software supplied by the tensile tester manufacturer.

To calculate the nominal shear adhesion strength, τ_a, from experimental data, following equation was used:

$$\tau_a = F_{max}/(\pi dL) \tag{1}$$

where F_{max} is the measured load at failure, *d* is the diameter of the FRC rod specimen and *L* is the adhesive joint length [25].

SEM *Philips 30* (*Philips*, Czech Republic) was used to inspect the loci of failure in order to ascertain the possible mechanisms of fracture. Specimens were gold-sputtered prior to placing in the SEM chamber. Micrographs were taken at different magnifications in order to provide an overview of each fractured area. Based on these observations, description of the failure mode has been attempted.

3. Results and discussion

The mean nominal shear adhesion strength, τ_a, determinated as an average from five measurements, and its standard deviation are given in the Table 2 for all investigated compositions and geometries. The effect of nanoparticle volume fraction, v_f, on the τ_a is illustrated in Fig. 2. Fig. 3 shows significant differences between composites containing either unidirectional or multidirectional oriented fibers. SEM micrographs of the three modes of failure observed are depicted in Fig. 4. Upper portion of the figures show original surface of the FRC rod.

The τ_a obtained for the specimen group I, where the denture base resin ring was bound directly to the FRC rod (no adhesive interlayer) was significantly lower than that for the joints with adhesive interlayer and also exhibited substantial data scatter. Poor wetting of the FRC rod surface with high viscosity denture base resin with granular morphology resulted in a very defective interface and, thus, in formation of a poor adhesion bond and failure at the FRC/denture base interface. The granular morphology is the consequence of the way denture base resin dough is prepared by mixing liquid monomer with polymer beads. The beads are swollen with the liquid monomer which homopolymerizes during

cure, hence, there is not enough unreacted double bonds to react with the reactive pendant groups on the surface of the FRC rod. Thus, the granular morphology causes very uneven contact of the denture base dough with the FRC surface (Fig. 4a).

The second group of specimens (II) had the same geometry as group I (no adhesive interlayer), however, in this case, low viscosity monomer mixture was used instead of the denture base dough. In addition, up to 8 vol.% (16 wt.%) of nanometer sized silica filler was incorporated in the monomer mixture to investigate its effect on the adhesion strength. The τ_a measured for this group of specimens was always significantly higher than that measured for the group I. For the joint length of 3 and 5 mm, the τ_a was 28 and 21 MPa, respectively. The τ_a was almost independent of the filler content. The slight decrease of τ_a with filler volume fraction, v_f, can be attributed to the reduction of the polymerization shrinkage with addition of silica resulting in lower normal clamping stress at the ring/rod interface. Most probably, mechanical interlocking with interfacial chemical bonding is the actual mechanism of bonding between the ring and FRC [26]. Good wetting of the FRC rod surface with the monomer mixture, even when filled with up
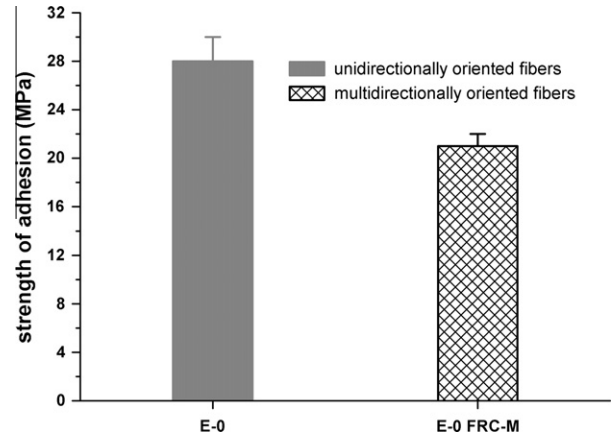
Fig. 3. Effect of fiber architecture on shear adhesion strength.

to 8 vol.% of fumed silica, formed significantly larger contact area compared to granular high viscosity denture base dough in
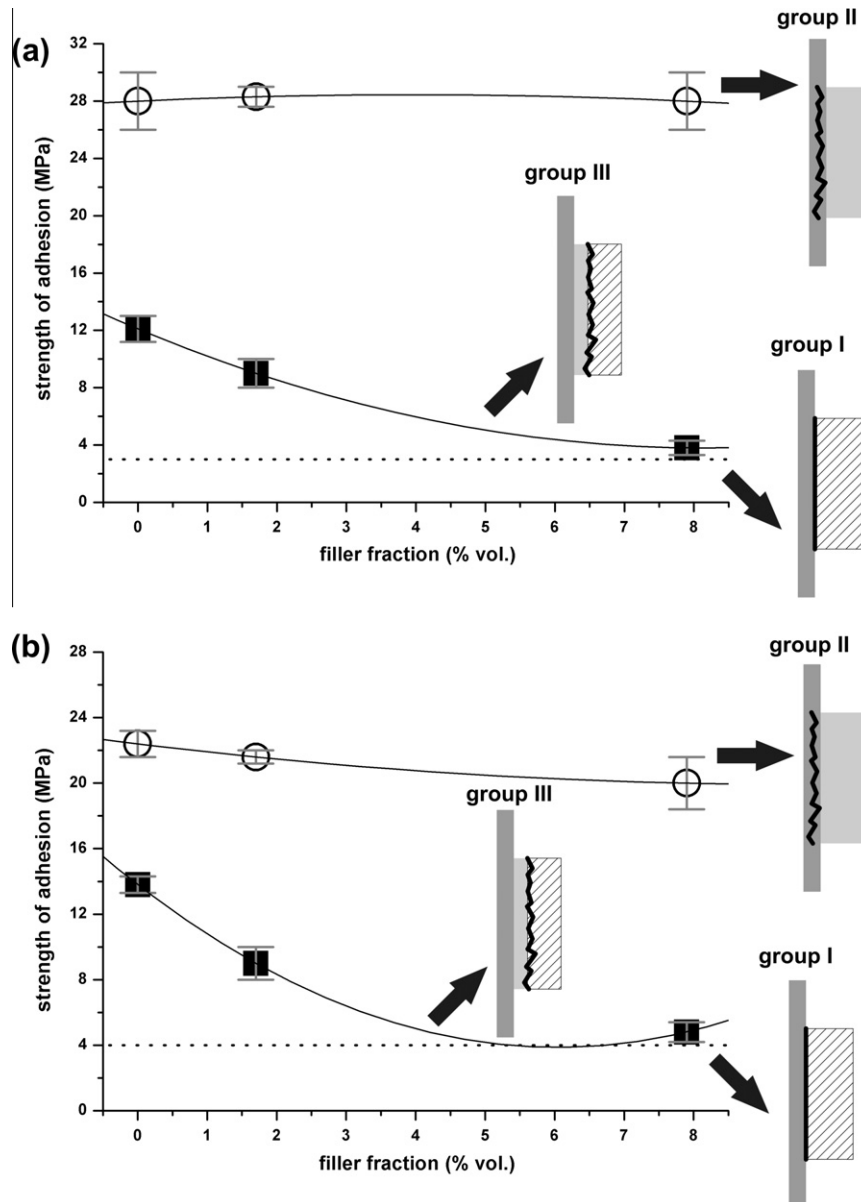
Fig. 2. The dependence of adhesion strength on filler fraction for two adhesive joint length (a) 3 and (b) 5 mm.
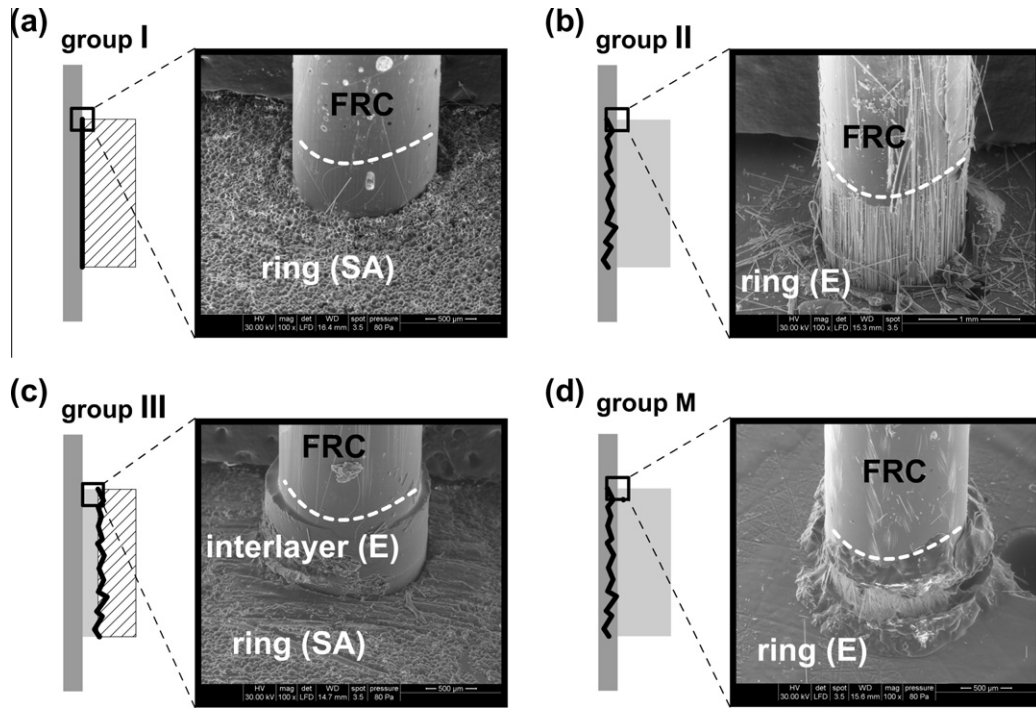
Fig. 4. Schematic illustration and SEM micrograph of fracture surface of (a) group I: SA, (b) group II: E-0, (c) group III: SAE-0 and (d) group M: E-0 FRC-M.
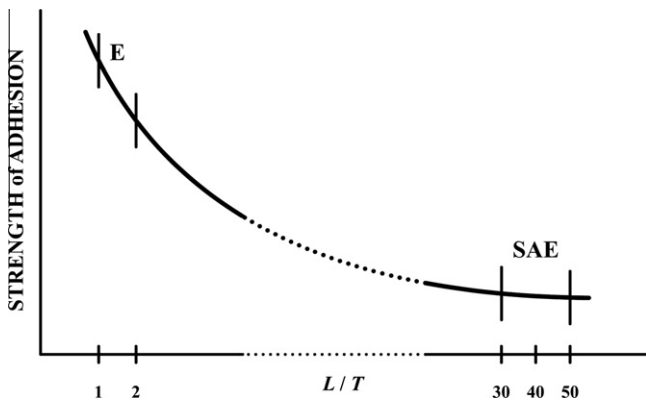
Fig. 5. The dependence of adhesion strength on the L/T ratio, where L is adhesive joint length and T is thickness of interlayer [29].
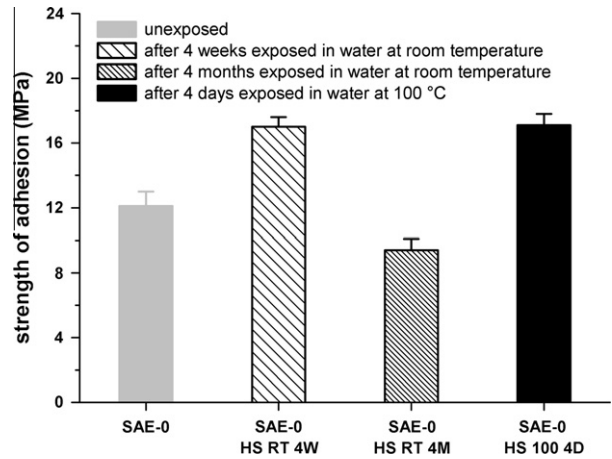
Fig. 6. Adhesion strength before and after the exposure to the moist environment.

Table 3
Adhesion strength of materials studied before and after the exposure to the moist environment.

Group	Subgroup	Shear adhesion strength, τ_a (MPa)
III	SAE-0	12.1 ± 0.9
HS	SAE-0 HS RT 4 W	17.0 ± 0.6
	SAE-0 HS RT 4 M	9.4 ± 0.7
	SAE-0 HS 100 4D	17.1 ± 0.7

samples of group I. As confirmed by the SEM, the interlaminar shear failure of the FRC rod becomes the mechanism that is limiting the shear adhesion strength of this type of joint regardless of the joint length (Fig. 4b).

The dimethacrylate resin used in both FRC and ring was identical and should promote formation of chemical bond between the FRC surface and ring. In addition, light cured FRC rod surface

may still contain a number of unreacted C═C groups, especially in the case, when light cure was performed without presence of oxygen. It was reported, that polymerization of C═C bonds in a light cured composite continue for at least 24 h after exposure to light [27]. It seems reasonable to assume that there were a number of unreacted double bonds on the surface of cured FRC rod, which could allow formation of covalent bonds between ring and FRC. Observations of the surface of cured FRC rods revealed that there was always a resin rich layer with no fibers protruding to the surface to provide additional means of bonding. Moreover, monomer from the ring may partly swell the surface resin rich layer of the FRC resulting in formation of strong interphase layer. On the other hand, the precise mechanism of interfacial bonding was far less important in controlling the adhesion strength of the joint than the mechanical properties of the ring and FRC [24].

In the specimen group III, where the adhesive interlayer of varying composition was used, the adhesion strength was lower

compared to the group II discussed above and τ_a decreased with increasing filler volume fraction, v_f, significantly, from 12 to 4 MPa. The difference between τ_a for the two joint lengths was statistically insignificant. Presence of the adhesive interlayer moved the loci of the joint failure to the interlayer/denture base ring interface. As expected from the results on specimens of group II, increasing of the silica content did not reduce the adhesion strength of the interlayer/FRC interface. Hence, the strong decrease of the adhesion strength between the interlayer and denture base ring with increasing v_f was caused by the increase of the viscosity of the adhesive interlayer compound. SEM micrographs showed that the crack path runs through interface denture base ring/adhesive interlayer (Fig. 4c). The manner in which the failure propagated after initiation was the same for both unidirectional and multidirectional reinforced FRC substrate, but the joint with braided fibers (group M) showed lower strength of adhesion. This decrease can be attributed to lower tensile strength of E-glass fibers and to the difference in the orientation of the braided fibers against the external loading. It can be seen from Fig. 4d that matrix material has been removed from the surface, leading to exposing of the braided fibers. The SEM fractographs confirmed the prediction of the crack path that has been previously proposed using a simple fracture mechanics model [26] (Fig. 4).

Effect of the area of the adhesive joint on adhesion strength was investigated using two joint lengths of 3 and 5 mm. For a given areas of adhesive joint, the ultimate load of the joint increases as the bonded length increase. However, the average bond strength decreases, due to the non-uniform distribution of the bond stresses along the bonded length [28]. This trend occurred only in case of the group II. In case of the groups of specimens with interlayer,

shear bond strength was almost independent on area of adhesive joint. This fact is explained based on the analogy described in literature [29]. Fig. 5 shows the dependence of adhesion strength on the joint length/interlayer thickness ratio (L/T). In case of groups of specimens without interlayer – group II, L/T ratio is equal to 0.916 (3/3.275) for adhesive joint length 3 mm. For adhesive joint length 5 mm is L/T ratio equal to 1.527 (5/3.275). They are situated in the part of curve, where shear bond strength decrease rapidly with L/T ratio. On the other hand, in case of groups of specimens with interlayer – group III – L/T ratio is equal to 30 (3/0.1) for adhesive joint length 3 mm and for length 5 mm is equal to 50 (5/0.1). They are situated in the part of curve, where shear bond strength is practically independent on adhesive joint length.

The change of the τ_a for the specimens with unfilled adhesive interlayer (group III) after the exposure to the moist environment at 23 °C for up to 4 months and accelerated hydrolytic degradation at 100 °C for 4 days was investigated (Table 3, Fig. 6). After 4 weeks, the τ_a increased to 17 MPa compared to the 12 MPa measured immediately after curing the joint. Further exposure of the joint led to a gradual decrease of the τ_a to 9 MPa after 16 weeks. Interestingly, the accelerated hydrolytic degradation of the joint at 100 °C for 100 h resulted as well in an increase of the τ_a to 17 MPa. The τ_a enhancement was attributed to the increase of toughness of the interphase region by penetration of water molecules into the cured resin [24,30–32]. This may result in its partial swelling, thus, relaxing portion of internal stresses as well as locally enhancing segmental mobility. Water molecules act as a plasticizer and the polymer chains generally become more mobile. This is in agreement with previous published data [24]. SEM micrograph showed crack entering the FRC rod (Fig. 7a and c).
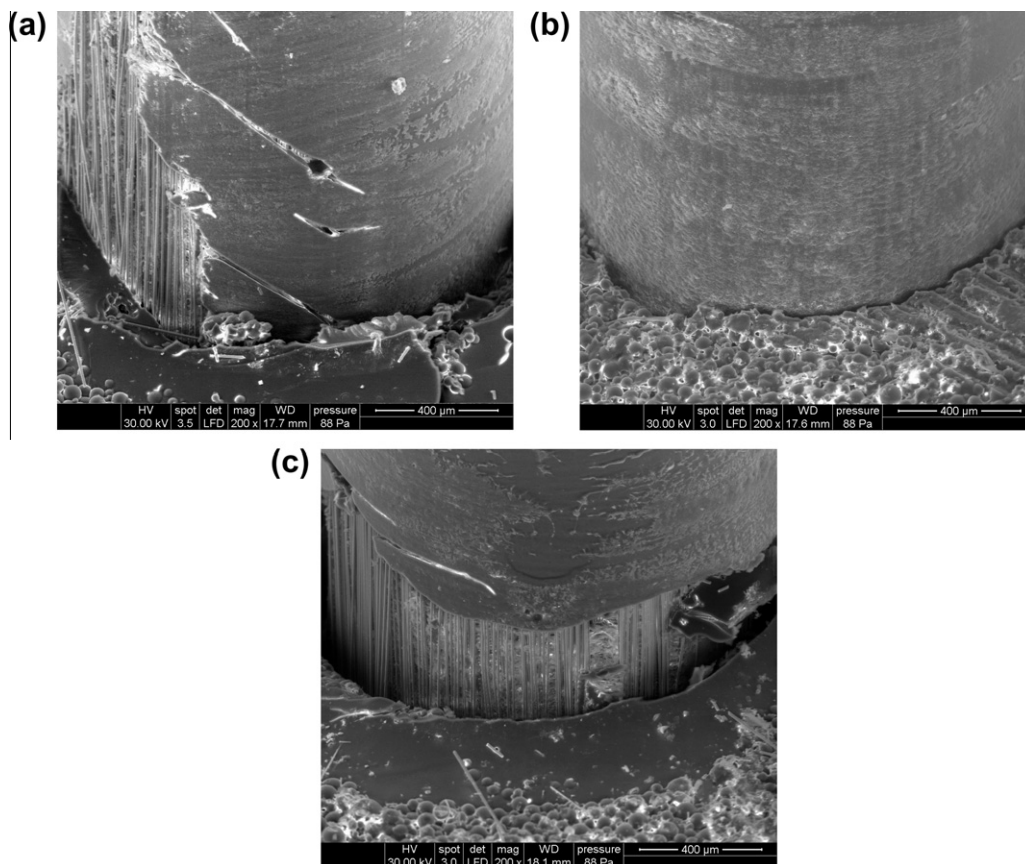
Fig. 7. SEM micrographs of the fracture surfaces: (a) after 4 weeks exposed in water at room temperature (SAE-0 HS RT 4 W), (b) after 4 months exposed in water at room temperature (SAE-0 HS RT 4 M) and (c) after 4 days exposed in water at 100 °C (SAE-0 HS 100 4D).

Failure was a mixture of interfacial crack and interlaminar failure. On the other hand, there was noticeable decrease of τ_a in system after exposure to distilled water at room temperature for 16 weeks. One possible explanation is that after reaching swelling equilibrium at given temperature and pressure, water diffusing into the joint becomes located preferentially at the interface. Here, it can hydrolyze existing hydrogen bonds and act as a lubricant, thus reducing the τ_a. In Fig. 7b, fracture surface is seen to be without interlaminar failure. Loci of failure was between interlayer/denture base ring interface.

4. Conclusions

In this study, adhesion strength between FRC based on dimethacrylate matrix and PMMA denture/base resin lightly crosslinked with dimethacrylate was investigated using specially modified pull-out test. The influence of the architecture of the FRC substrate and the adhesive interlayer composition on the shear adhesion strength was investigated for fresh and hydrolytically aged joints.

Strength of adhesion between FRC and acrylic denture-base resin without interlayer was weak due to poor wetting of the surface of FRC rod, resulting in poor conditions for formation of adhesion bonds. However, when interlayer was used, adhesion strength increased. This can be explained based on better wetting of the surface of FRC rod resulting in suitable conditions for formation of covalent bonds between the ring and rod. Limiting value was the interface interlayer/ring and higher viscosity of adhesive filled with nanofiller. On the other hand, the highest adhesion strength was achieved for adhesive itself. However, the limiting value was fiber architecture and interlaminar shear strength of the FRC composite. Mode of failure in adhesive joints was heavily dependent on environmental conditions.

Acknowledgment

References

[1] Narva KK, Lassila LV, Vallittu PK. The static strength and modulus of fiber reinforced denture base polymer. Dent Mater 2005;21:421–8.
[2] Craig R, ÓBrien WJ, Powers JM. Dental materials – properties and manipulation. Mosby, Year Book; 1992.
[3] Behr M, Rosentritt M, Leibrock A, Schneider-Feyrer S, Handel G. In vitro study of fracture strength and marginal adaptation of fibre-reinforced adhesive fixed partial inlay dentures. J Dent 1999;27:161–8.
[4] Cadiou D, Grundler T. Le concept Targis®–Vectris®, 2eme partie. Proth Dent 1997;124:27–31.
[5] Chow TK. Ultra-high-modulus polyethylene fibres in denture construction. In: Vallittu PK. The first international symposium on fibre reinforced plastics in dentistry, 27–29 August 1998, Turku, Finland. University of Turku, Institute of Dentistry and Biomaterials Project; 1999.
[6] Freilich MA, Karmaker AC, Burstone CJ, Goldberg AJ. Development and clinical applications of a light-polymerized fiber-reinforced composite. J Prosthet Dent 1998;80:311–8.
[7] Goldberg AJ. Material design and clinical experience with fibre composites in dentistry. In: Vallittu PK. The first international symposium on fibre reinforced plastics in dentistry, 27–29 August 1998, Turku, Finland. University of Turku, Institute of Dentistry and Biomaterials Project; 1999.
[8] Gutteridge DL. Reinforcement of poly(methyl methacrylate) with ultra-high-modulus polyethylene fibre. J Dent 1992;20:50–4.
[9] Karmaker AC, DiBenedetto AT, Goldberg AJ. Continuous fiber reinforced composite materials as alternatives for metal alloys used for dental appliances. J Biomater Appl 1997;1:318–28.
[10] Loose M, Rosentritt M, Leibrock A, Behr M, Handel G. In-vitro study of fracture strength and marginal adaptation of fibre-reinforced composite versus all ceramic fixed partial dentures. Eur J Prosthodont Restor Dent 1998;6:55–62.
[11] Unterbrink G. Vectris fibre composite system for fixed prosthodontics. In: Vallittu PK. The first symposium on fibre reinforced plastics in dentistry, 27–29 August 1998, Turku, Finland. University of Turku, Institute of Dentistry and Biomaterials Project; 1999.
[12] Goldberg AJ, Burstone CJ. The use of continuous fiber reinforcement in dentistry. Dent Mater 1992;8:197–202.
[13] Behr M, Rosentritt M, Lang R, Handel G. Flexural properties of fiber reinforced composite using a vacuum/pressure or a manual adaptation manufacturing process. J Dent 2000;28:509–14.
[14] Issac DH. Engineering aspects of the structure and properties of polymer–fibre composites. In: Vallittu PK. The first international symposium on fibre reinforced plastics in dentistry, 27–29 August 1998, Turku, Finland. University of Turku, Institute of Dentistry and Biomaterials Project; 1999.
[15] Vallittu PK. Experiences of using glass fibres with multiphase acrylic resin systems. Theoretical background and clinical examples. In: Vallittu PK. The first international symposium on fibre reinforced plastics in dentistry, 27–29 August 1998, Turku, Finland. University of Turku, Institute of Dentistry and Biomaterials Project; 1999.
[16] Freilich M, Meiers JC, Duncan JP, Goldberg AJ. Fiber-reinforced composites in clinica. Dentistry Quintessence Publishing; 2000.
[17] Lastumaki TM, Kallio TT, Vallittu PK. The bond strength of light-curing composite resin to finally polymerized and aged glass fiber-reinforced composite substrate. Biomaterials 2002;23:4533–9.
[18] Nicholson JW. Adhesive dental materials – a review. Int J Adhes Adhes 1998;18:229–36.
[19] Jancar J. Bond strength of five dental adhesives using a fracture mechanics approach. J Mech Behav Biomed 2011;4:245–54.
[20] Jancar J, Wang W, DiBenedetto AT. On the heterogenous structure of thermally cured bis-GMA/TEGDMA resins. J Mater Sci – Mater Med 2000;11:675–82.
[21] Stansbury JW, Trujillo-Lemon M, Lu H, Ding X, Lin Y, Ge J. Conversion-dependent shrinkage stress and strain in dental resins and composites. Dent Mater 2005;21:56–67.
[22] Jancar J, Hynstova K, Pavelka V. Toughening of denture base resin with short deformable fibers. Comp Sci Technol 2009;69:457–62.
[23] Donato RK, Matejka L, Schrekker HS, Plestil J, Jigounov A, Brus J, et al. The multifunctional role of ionic liquids in the formation of epoxy–Silica nanocomposites. J Mater Chem 2011;21:13801–10.
[24] Polacek P, Jancar J. Effect of filler content on the adhesion strength between UD fiber reinforced and particulate filled composites. Comp Sci Technol 2008;68:251–9.
[25] Wilson HJ. Resin-based restoratives. Br Dent J 1998;164:326–31.
[26] DiBenedetto AT, Conelly SM, Lee WC, Accorsi M. The properties of organosilane/polyester interfaces at an E-glass fiber surface. J Adhes 1995;52:41–64.
[27] Keski-Nikkola MS, Alander PM, Lassila LVJ, Vallittu PK. Bond strength of Gradia® veneering composite to fiber-reinforced composite. J Oral Rehab 2004;31:1178–83.
[28] Lorenzis L, Rizzo A, La Tegola AA. Modified pull-out test for bond of near-surface mounted FRP rods in concrete. Compos Part B – Eng 2002;33:589–603.
[29] Pocius AV. Adhesion and adhesives technology: an introduction. Hanser; 2002.
[30] Bouillaguet S et al. Hydrothermal and mechanical stresses degrade fiber–matrix interfacial bond strength in dental fiber-reinforced composites. J Biomed Matter Res Part B: Appl Biomater 2006;76B:98–105.
[31] Gohring TN, Gallo L, Luthy H. Effect of water storage, thermocycling, the incorporation and site of placement of glass-fibers on the flexural strength of vennering composite. Dent Mater 2005;21:761–72.
[32] Lassila LVJ, Nohrström T, Vallitu PK. The influence of short-term water storage on the flexural properties of unidirectional glass fiber-reinforced composites. Biomaterials 2002;23:2221–9.